

# Spectral functions, Fermi surface and pseudo gap in the $t$ - $J$ model

P. Prelovšek and A. Ramšak

*Faculty of Mathematics and Physics, University of Ljubljana, 1111 Ljubljana, Slovenia*

*J. Stefan Institute, University of Ljubljana, 1111 Ljubljana, Slovenia*

(September 4, 2001)

Spectral functions within the generalized  $t$ - $J$  model as relevant to cuprates are analyzed using the method of equations of motion for projected fermion operators. In the evaluation of the self energy the decoupling of spin and single-particle fluctuations is performed. It is shown that in an undoped antiferromagnet (AFM) the method reproduces the selfconsistent Born approximation. For finite doping with short range AFM order the approximation evolves into a paramagnon contribution which retains large incoherent contribution in the hole part of the spectral function as well as the hole-pocket-like Fermi surface at low doping. On the other hand, the contribution of (longitudinal) spin fluctuations, with the coupling mostly determined predominantly by  $J$  and next-neighbor hopping  $t'$ , is essential for the emergence of the pseudogap. The latter shows at low doping in the effective truncation of the large Fermi surface, reduced electron density of states and at the same time quasiparticle density of states at the Fermi level.

PACS numbers: 71.27.+a, 72.15.-v, 71.10.Fd

## I. INTRODUCTION

One of the central issues in the experimental and theoretical investigations of superconducting cuprates is the understanding of low-energy electronic excitations in these compounds [1], where the clue to their high-temperature superconductivity lies possibly already in their anomalous normal-state properties. In recent years, in particular, the remarkable progress in the angle-resolved photoemission spectroscopy (ARPES) experiments revealed quite universal development of electron spectral properties as a function of doping. In most investigated  $\text{Bi}_2\text{Sr}_2\text{CaCu}_2\text{O}_{2+\delta}$  (BSCCO) ARPES shows quite well defined large Fermi surface in the overdoped and optimally doped samples at  $T > T_c$ , whereby the low-energy behavior with increasing doping in the overdoped regime qualitatively approaches (but does not in fact reach) that of the normal Fermi-liquid with underdamped quasiparticle (QP) excitations. On the other hand, in the underdoped materials the QP dispersing through the Fermi surface (FS) are resolved by ARPES in BSCCO only in parts of the large FS, in particular along the nodal  $(0, 0)$ - $(\pi, \pi)$  direction [2], indicating that the rest of the large FS is truncated [3], i.e. either fully or effectively gaped. At the same time near the  $(\pi, 0)$  momentum ARPES reveals a hump at  $\sim 100$  meV [2], which indicates on the existence of the pseudogap scale, which is consistent with the characteristic temperature pseudogap scale  $T^* > T_c$ , which appears also as a crossover in several other quantities: uniform susceptibility  $\chi(T)$ , resistivity  $\rho(T)$ , the specific heat  $C_V(T)$  and the Hall constant  $R_H(T)$  [1]. Although the latter anomalies in thermodynamic and transport quantities are quite similar (or even better confirmed and more pronounced) also in  $\text{La}_{2-x}\text{Sr}_x\text{Cu}_2\text{O}_4$  (LSCO), spectral properties of the latter [4] are qualitatively different from BSCCO, pre-

sumably due to the crucial role of stripe structures in the LSCO in the regime of intermediate doping.

Since electron spectral functions are the central quantity to characterize and understand anomalous Fermi liquid in cuprates, they have been the subject of numerous theoretical studies. There appears to be at least a theoretical consensus on the spectral functions in an undoped reference antiferromagnet (AFM), describing a single hole inserted in an AFM behaving in two-dimensional (2D) planar system as a QP with strongly renormalized mass and large incoherent component. The spectral function is well captured within the selfconsistent Born approximation (SCBA) [5] for the simplest relevant  $t$ - $J$  model, whereby for an agreement with experiments on undoped cuprates, i.e.,  $\text{Sr}_2\text{CuO}_2\text{Cl}_2$  [6] and  $\text{Ca}_2\text{CuO}_2\text{Cl}_2$  [7] longer range hopping terms have been invoked [8,9].

For larger (finite) doping in the lack of reliable analytical techniques numerical approaches have been used extensively. Starting with the simplest models for correlated electrons in cuprates, i.e., the Hubbard model and the  $t$ - $J$  models on planar lattices, numerical studies employing mainly the exact-diagonalization and the quantum Monte Carlo methods were able to confirm some gross features consistent with experiments. In particular this includes: a) the existence of the large FS already in moderately doped AFM [10,8], b) the overdamped character of QP at the intermediate doping [11,12], consistent with the marginal Fermi-liquid concept [13], c) the pseudogap features at lower doping in spectral functions [14] and in the density of states (DOS) [12], and d) quite visible contribution of longer range hopping [9]. Whereas numerical studies confirm the relevance of simplest models and results for cuprates, still they are prevented to approach effectively the low-energy regime and results need a proper analytical (phenomenological) interpretation.

Analytical approximations to spectral properties of relevant models for 2D systems at finite doping have proven to be very delicate due to strong interaction between electron excitations, spin degrees and pairing fluctuations. For the one-band Hubbard model spectral functions have been evaluated within the random-phase approximation for AFM fluctuations [15] and within the self-consistent conserving (FLEX) theory [16], both restricted to modest  $U/t$ . Starting with the  $t$ - $J$  model strong correlations are explicitly taken into account in slave boson theories [17], where it is however difficult to incorporate AFM spin fluctuations. The latter play the essential role in phenomenological theory of the spin-fermion model leading to the nearly AFM Fermi liquid [18]. Recently aspects of the pseudogap features in the underdoped regime have been found in this model evaluating the self energy involving a strong coupling to AFM spin fluctuations [19,20].

Concerning the origin and the explanation of the pseudogap scale it seems plausible that at low doping it is related to the exchange  $J$  since  $T^* \sim J$  in low-doping materials, whereas it merges  $T^* \sim T_c$  in optimally doped samples. This indicates on the importance of AFM spin correlations for the emergence of the (large) pseudogap as found also in the numerical studies [14,11,12] and in phenomenological model studies [19,20]. The renormalization group studies of the Hubbard model [21] (with moderate  $U/t$ ) also reveal the instability of the normal Fermi liquid close to the half-filled band (insulator) and a possible truncation of the Fermi surface, but here either the spin or pairing fluctuations can take the dominant role depending on FS nesting conditions whereby the longer-range hopping terms can be quite important.

One of present authors introduced the equations-of-motion (EQM) method [22] for the evaluation of the spectral functions within the  $t$ - $J$  model. It has been shown that EQM for projected fermionic operators implicitly reveal an effective spin-fermion coupling. Using the simplest decoupling it was possible to relate the overdamped marginal-type character of QP to the marginal dynamics of spins [22] but also to treat the superconducting fluctuations and transition [23]. EQM method has been also applied for the Hubbard model [24]. The analysis of spectral functions within the  $t$ - $J$  model has been recently improved [25] by more appropriate treatment of the self energy by dealing separately with: a) the strong coupling to transverse short-range AFM spin fluctuations - paramagnons and b) the moderate coupling to slower longitudinal fluctuations of the AFM order parameter. The theory and results were partially presented already in Ref. [25]. The aim of this paper is to present the theory and in particular its consequences and results in more detail. The main advantage of this theory is that it allows for the study of the evolution of spectral function as a function of doping: from an undoped system up to moderate doping. The emphasis is on the results at  $T = 0$ , in particular on: a) the development of the FS from a

hole-pocket like into a large one, b) the emergence of the pseudogap in the spectral function and related effective truncation of the FS most pronounced near  $(\pi, 0)$  in the Brillouin zone, c) anomalous properties of QP at the FS remaining well defined even in the pseudogap regime, d) depleted DOS and moreover the quasiparticle DOS (related to specific heat coefficient) with doping.

The paper is organized as follows: In Sec. II EQM method for the spectral function within the  $t$ - $J$  model is summarized. Sec. III is devoted to the evaluation of the self energy within the decoupling approximation separately treating the paramagnon contribution  $\Sigma_{\text{pm}}$  and the contribution of longitudinal spin fluctuations  $\Sigma_{\text{lf}}$ . In Sec. IV results of the simplified analysis of the pseudogap features are presented taking into account an effective renormalized band and explicitly  $\Sigma_{\text{lf}}$ . Sec. V presents results of the full selfconsistent solution for spectral function as a function of doping.

## II. EQUATIONS OF MOTION

In order to take explicitly into account strong correlations we study the  $t$ - $J$  model,

$$H = - \sum_{i,j,s} t_{ij} \tilde{c}_{js}^\dagger \tilde{c}_{is} + J \sum_{\langle ij \rangle} (\mathbf{S}_i \cdot \mathbf{S}_j - \frac{1}{4} n_i n_j), \quad (1)$$

where fermionic operators are projected ones not allowing for the double occupancy of sites, i.e.,

$$\tilde{c}_{is}^\dagger = (1 - n_{i,-s}) c_{is}^\dagger. \quad (2)$$

Since longer range hopping appears to be important for the proper description of spectral function in cuprates, both for the shape of the FS at optimum doping materials [9] as well as for the explanation of ARPES of undoped insulators [6,7,9], we consider besides  $t_{ij} = t$  for the n.n. hopping also  $t_{ij} = t'$  for the n.n.n. hopping on a square lattice.

Our goal is to evaluate the electron Green's function (propagator) directly for projected fermionic operators,

$$\begin{aligned} G(\mathbf{k}, \omega) &= \langle\langle \tilde{c}_{\mathbf{k}s}; \tilde{c}_{\mathbf{k}s}^\dagger \rangle\rangle_\omega = \\ &= -i \int_0^\infty e^{i(\omega+\mu)t} \langle\langle \tilde{c}_{\mathbf{k}s}(t), \tilde{c}_{\mathbf{k}s}^\dagger \rangle\rangle_+ dt, \end{aligned} \quad (3)$$

which is equivalent to the usual propagator within the allowed basis states of the model, Eq. (1). In the EQM method [26] one uses relations for general correlation functions

$$\begin{aligned} \omega \langle\langle A; B \rangle\rangle_\omega &= \langle\langle A, B \rangle\rangle_+ + \langle\langle [A, H]; B \rangle\rangle_\omega = \\ &= \langle\langle A, B \rangle\rangle_+ - \langle\langle A; [B, H] \rangle\rangle_\omega. \end{aligned} \quad (4)$$

and applies the propagator  $G(\omega) = \langle\langle A; A^\dagger \rangle\rangle_\omega$ . If we define the (orthogonal) operator  $C$  as

$$[A, H] = \zeta A - iC, \quad \langle \{C, A^\dagger\}_+ \rangle = 0, \quad (5)$$

we can express

$$G(\omega) = G_0(\omega) + \frac{1}{\alpha^2} G_0(\omega)^2 \langle \langle C; C^\dagger \rangle \rangle_\omega, \quad (6)$$

$$G_0(\omega) = \frac{\alpha}{\omega - \zeta}, \quad \alpha = \langle \{A, A^\dagger\}_+ \rangle.$$

Identifying the self energy  $\Sigma(\omega)$  as the irreducible part of  $\langle \langle C; C^\dagger \rangle \rangle_\omega$  we can express Eq. (6) as

$$G(\omega) = \frac{\alpha}{\omega - \zeta - \Sigma(\omega)}, \quad \Sigma(\omega) \sim \frac{1}{\alpha} \langle \langle C; C^\dagger \rangle \rangle_\omega^{irr}. \quad (7)$$

Within the diagrammatic technique  $\Sigma(\omega)$  corresponds to the contribution of irreducible diagrams. Generally  $\Sigma(\omega)$  can be defined as a memory function within the Mori projection method [27]. Anyway, in most cases the successful application of the method relies on the appropriate decoupling or other approximation of the memory function  $\Sigma(\omega)$  [28].

Applying the formalism to the propagator, Eq. (3), we have to deal with the EQM for  $\tilde{c}_{\mathbf{k}s}^\dagger$  with a nontrivial normalization factor,

$$\alpha = \frac{1}{N} \sum_i \langle \{ \tilde{c}_{is}, \tilde{c}_{is}^\dagger \}_+ \rangle = 1 - \frac{c_e}{2} = \frac{1}{2}(1 + c_h). \quad (8)$$

By taking explicitly into account the projection in Eq. (2) the EQM follow,

$$[\tilde{c}_{is}, H] = - \sum_j t_{ij} [(1 - n_{i,-s}) \tilde{c}_{js} + S_i^\mp \tilde{c}_{j,-s}] + \frac{1}{4} J \sum_{j \text{ n.n. } i} (2s S_j^z \tilde{c}_{is} + 2S_j^\mp \tilde{c}_{i,-s} - n_j \tilde{c}_{is}) \quad (9)$$

with  $s = \pm 1$ . We express 'bosonic' variables in to terms of spin and density operators, i.e.,  $n_{i,-s} = n_i/2 - s S_i^z$ . Assuming as well that we are dealing with a paramagnetic metal with  $\langle \mathbf{S}_i \rangle = 0$  and a homogeneous electron density  $\langle n_i \rangle = c_e$ , we get

$$-iC_{\mathbf{k}s} = [\tilde{c}_{\mathbf{k}s}, H] - \zeta_{\mathbf{k}} \tilde{c}_{\mathbf{k}s}, \quad (10)$$

and

$$[\tilde{c}_{\mathbf{k}s}, H] = [(1 - \frac{c_e}{2}) \epsilon_{\mathbf{k}}^0 - J c_e] \tilde{c}_{\mathbf{k}s} + \frac{1}{\sqrt{N}} \sum_{\mathbf{q}} m_{\mathbf{kq}} [s S_{\mathbf{q}}^z \tilde{c}_{\mathbf{k}-\mathbf{q},s} + S_{\mathbf{q}}^\mp \tilde{c}_{\mathbf{k}-\mathbf{q},-s} - \frac{1}{2} \tilde{n}_{\mathbf{q}} \tilde{c}_{\mathbf{k}-\mathbf{q},s}], \quad (11)$$

where  $\tilde{n}_i = n_i - c_e$ ,  $m_{\mathbf{kq}}$  is the effective spin-fermion coupling,

$$m_{\mathbf{kq}} = 2J\gamma_{\mathbf{q}} + \epsilon_{\mathbf{k}-\mathbf{q}}^0 \quad (12)$$

and  $\epsilon_{\mathbf{k}}^0$  is the bare band dispersion, i.e., for the model (1) on a square lattice

$$\epsilon_{\mathbf{k}}^0 = -4t\gamma_{\mathbf{k}} - 4t'\gamma'_{\mathbf{k}}, \quad (13)$$

$$\gamma_{\mathbf{k}} = \frac{1}{2}(\cos k_x + \cos k_y), \quad \gamma'_{\mathbf{k}} = \cos k_x \cos k_y.$$

Equations (4),(11),(13) define also the 'renormalized' band

$$\zeta_{\mathbf{k}} = \frac{1}{\alpha} \langle \{ [\tilde{c}_{\mathbf{k}s}, H], \tilde{c}_{\mathbf{k}s}^\dagger \}_+ \rangle = \bar{\zeta} - 4\eta_1 t \gamma_{\mathbf{k}} - 4\eta_2 t' \gamma'_{\mathbf{k}}, \quad (14)$$

$$\eta_j = \alpha + \frac{1}{\alpha} \langle \mathbf{S}_0 \cdot \mathbf{S}_j \rangle,$$

where  $\eta_j$  are determined solely by short range spin correlations and  $\bar{\zeta}$  is a  $\mathbf{k}$  independent term (still dependent on various static correlations).

Above quantities determine the propagator

$$G(\mathbf{k}, \omega) = \frac{\alpha}{\omega + \mu - \zeta_{\mathbf{k}} - \Sigma(\mathbf{k}, \omega)}, \quad (15)$$

and the corresponding spectral function  $A(\mathbf{k}, \omega) = -(1/\pi) \text{Im}G(\mathbf{k}, \omega)$ , provided that we find a method to evaluate  $\Sigma(\mathbf{k}, \omega)$ .

### III. SELF ENERGY

#### A. Undoped antiferromagnet

It is desirable that in the case of an undoped AFM our treatment of  $\Sigma$  and the spectral function reproduces quite successful SCBA equations [5] for the Green's function of a hole in an AFM. Let us concentrate here on the relevant n.n. hopping, since the  $t'$  term represents a hopping on the same sublattice within an ordered AFM and is therefore nearly free. For the SCBA the reference state is the Néel state with  $n_{is} = 0, 1$  for  $i = A, B$  sublattices, respectively, and the SCBA effective Hamiltonian can be written as

$$H_h = -t \sum_{\langle ij \rangle} (h_i h_j^\dagger a_j + h_j h_i^\dagger a_j^\dagger) + H_J, \quad (16)$$

where  $h_i$  represent holon operators and  $a_i$  spin flip operators. The corresponding holon EQM then follows from Eq. (16)

$$-i \frac{d}{dt} h_i^\dagger = [h_i, H_h] = t \sum_{j \text{ n.n. } i} h_j^\dagger (a_i^\dagger + a_j). \quad (17)$$

It is now straightforward to establish the relation of Eq. (17) with the EQM for  $\tilde{c}_{is}$  by considering one Néel sublattice  $i = A$  with the reference state  $n_{is} = 1$ . In this case  $1 - n_{i,-s} = 1$  and by formally replacing  $\tilde{c}_{js} = \tilde{c}_{j,-s} S_j^\mp$  we get by considering only the  $t$  term in Eq. (9),

$$i \frac{d}{dt} \tilde{c}_{is} \sim -t \sum_{j \text{ n.n. } i} (S_i^\mp + S_j^\mp) \tilde{c}_{j,-s}. \quad (18)$$

To be consistent with the SCBA we neglect here the  $J$  term in Eq. (9) since anyhow  $J \ll t$ . Within the linearized magnon theory EQM (17),(18) are formally identical, so we can furtheron follow the procedure of the evaluation of  $\Sigma_{\text{AFM}}(\mathbf{k}, \omega)$  within the SCBA to reproduce in the first place spectral properties of an undoped AFM. In this case we do not try to improve the SCBA, since the latter approximation is simple and yields both qualitatively and quantitatively good results consistent with numerical studies and experiments. For an ordered 2D AFM where relevant spin excitations are magnons with dispersion  $\omega_{\mathbf{q}}$  we therefore get

$$\Sigma_{\text{AFM}}(\mathbf{k}, \omega) = \frac{1}{N} \sum_{\mathbf{q}} M_{\mathbf{k}\mathbf{q}}^2 G(\mathbf{k} - \mathbf{q}, \omega + \omega_{\mathbf{q}}), \quad (19)$$

$$M_{\mathbf{k}\mathbf{q}} = 4t(u_{\mathbf{q}}\gamma_{\mathbf{k}-\mathbf{q}} + v_{\mathbf{q}}\gamma_{\mathbf{k}}),$$

with

$$u_{\mathbf{q}} = \sqrt{\frac{2J + \omega_{\mathbf{q}}}{2\omega_{\mathbf{q}}}}, \quad v_{\mathbf{q}} = -\gamma_{\mathbf{q}} \sqrt{\frac{2J - \omega_{\mathbf{q}}}{2\omega_{\mathbf{q}}}},$$

$$\omega_{\mathbf{q}} = 2J\sqrt{1 - \gamma_{\mathbf{q}}^2}. \quad (20)$$

Since in a Néel state we have  $\eta_1 = 0$  and hence the renormalized band vanishes, i.e.,  $\zeta_{\mathbf{k}} = 0$ , we reproduce the usual SCBA equations for the hole spectral function within the  $t$ - $J$  model. The inclusion of the n.n.n. hopping  $t'$  is also simple within the SCBA since within the Néel state it does not induce a coupling to spin flips in Eq. (9) and therefore enters  $G(\mathbf{k}, \omega)$ , Eq. (15), only via the band term  $\zeta_{\mathbf{k}} \sim \bar{\zeta} - 4t'\gamma'_{\mathbf{k}}$ . It should also be noted that in contrast to the usual SCBA our procedure deals directly with the electron propagator and not with an unphysical holon one. Moreover it allows a straightforward generalization to the case of finite doping.

## B. Short range transverse spin fluctuations

For finite doping  $c_h > 0$  we assume that spin fluctuations remain dominant at the AFM wavevector  $\mathbf{Q} = (\pi, \pi)$  with the characteristic inverse AFM correlation length  $\kappa = 1/\xi_{\text{AFM}}$ . The latter seems to be the case for BSCCO as well as  $\text{YB}_2\text{Cu}_3\text{O}_{6+x}$ , but not for LSCO with pronounced stripe and spin-density structures with  $\mathbf{q}_{\text{SDW}} \neq \mathbf{Q}$ . For the former case one can divide the spin fluctuations into two regimes with respect to  $\tilde{\mathbf{q}} = \mathbf{q} - \mathbf{Q}$ : a) For  $\tilde{q} > \kappa$  spin fluctuations are paramagnons, i.e., they are propagating like magnons and are transverse to the local AFM short-range spin ordering. Hence it make sense to use Eqs.(19),(20) to represent paramagnon contribution to the self energy restricting the sum to the regime  $\tilde{q} > \kappa$ . b) For  $\tilde{q} < \kappa$  spin fluctuations are essentially not propagating modes but critically overdamped so deviations

from the long range order are essential. Alternative approximations to  $\Sigma(\mathbf{k}, \omega)$  have to be used here, as discussed in Sec. III.C.

We should also take into account that the SCBA formalism has been derived for an undoped AFM, i.e., for a hole spectral function at  $\omega < 0$  where only (added) holes participate. Since we are dealing with  $c_h > 0$  we take into account the scattering of hole-like ( $\omega < 0$ ) QP by replacing full propagator  $G$  in Eq. (19) by the hole part  $G^-$ ,

$$G^{\mp}(\mathbf{k}, \omega) = \pm \int_{\mp\infty}^0 \frac{d\omega' A(\mathbf{k}, \omega')}{\omega - \omega'}, \quad (21)$$

However it is easy to see that an analogous contribution should arise from the electron-like QP with  $\omega > 0$ . At finite doping case we therefore generalize (at  $T = 0$ ) Eq. (19) into the paramagnon contribution,

$$\Sigma_{\text{pm}}(\mathbf{k}, \omega) = \frac{1}{N} \sum_{q, \tilde{q} > \kappa} [M_{\mathbf{k}\mathbf{q}}^2 G^-(\mathbf{k} - \mathbf{q}, \omega + \omega_{\mathbf{q}}) + M_{\mathbf{k}+\mathbf{q}, \mathbf{q}}^2 G^+(\mathbf{k} + \mathbf{q}, \omega - \omega_{\mathbf{q}})], \quad (22)$$

which would emerge from Eq. (18). The consequence of Eq. (22) is that in general  $\text{Im}\Sigma_{\text{pm}}(\mathbf{k}, \omega > 0) \neq 0$  so that also electron-like QP can be damped due to magnon processes. We do not consider here effects of  $T > 0$  which could be easily incorporated through the magnon occupation, but in most cases do not have a strong influence at low  $T < J$ .

Here we stress two features of our approximation for paramagnon contribution  $\Sigma_{\text{pm}}$ :

a) we are dealing with a strong coupling theory due to  $t > \omega_{\mathbf{q}}$  and a selfconsistent calculation of  $\Sigma_{\text{pm}}$  is required, b) resulting  $\Sigma_{\text{pm}}(\mathbf{k}, \omega)$  as well  $A(\mathbf{k}, \omega)$  as are at low doping quite asymmetric with respect to  $\omega = 0$ . As in an undoped AFM the hole part  $G^-$  with the weight  $\propto (1 - c_h)/2 \sim 1/2$  generates a large incoherent part in  $A(\mathbf{k}, \omega \ll 0)$ . On the other hand,  $G^+$  has less weight  $\propto c_h$  and consequently the scattering of electron QP is in general much less effective.

## C. Coupling to longitudinal spin fluctuations

Discussing the self energy at finite doping, Eq. (22) represents only one contribution and we have to reconsider EQM (10),(11). We note that at  $c_h > 0$   $C_{\mathbf{k}\mathbf{s}}$  contains a remainder of a 'free' term  $\propto \tilde{c}_{\mathbf{k}\mathbf{s}}$ , which should be however neglected when evaluating the 'irreducible' part entering  $\Sigma$ , Eq. (7). Considering within the simplest approximation only the mode-coupling terms in Eq. (11) we also neglect the coupling to density fluctuation  $\tilde{n}_{\mathbf{q}}$  which should contribute much less to  $\Sigma$  in the absence of charge ordering or charge instabilities at low doping.

Taking into account only spin fluctuations, at  $c_h > 0$  we are dealing with a paramagnet without an AFM long-range order and besides the paramagnon excitations also the coupling to longitudinal spin fluctuations become crucial. The latter restore the spin rotation symmetry in a paramagnet and EQM (11) naturally introduce such a spin-symmetric coupling. Assuming within a simplest approximation that the dynamics of fermions and spins is independent,

$$\langle S_{\mathbf{q}}^z(t) \tilde{c}_{\mathbf{k}-\mathbf{q},s}(t) S_{-\mathbf{q}}^z \tilde{c}_{\mathbf{k}-\mathbf{q}',s}^\dagger \rangle \sim \delta_{\mathbf{q}\mathbf{q}'} \langle S_{\mathbf{q}}^z(t) S_{-\mathbf{q}}^z \rangle \langle \tilde{c}_{\mathbf{k}-\mathbf{q},s}(t) \tilde{c}_{\mathbf{k}-\mathbf{q},s}^\dagger \rangle, \quad (23)$$

we get for the contribution of longitudinal fluctuations

$$\Sigma_{\text{lf}}(\mathbf{k}, \omega) = \frac{r_s}{\alpha} \sum_{\mathbf{q}} \tilde{m}_{\mathbf{k}\mathbf{q}}^2 \int \int \frac{d\omega_1 d\omega_2}{\pi} g(\omega_1, \omega_2) \frac{\tilde{A}(\mathbf{k}-\mathbf{q}, \omega_1) \chi''(\mathbf{q}, \omega_2)}{\omega - \omega_1 - \omega_2}, \quad (24)$$

$$g(\omega_1, \omega_2) = f(-\omega_1) + \bar{n}(\omega_2) = \frac{1}{2} \left[ \text{th} \frac{\beta\omega_1}{2} + \text{cth} \frac{\beta\omega_2}{2} \right],$$

where  $\chi$  is the dynamical spin susceptibility

$$\chi(\mathbf{q}, \omega) = -i \int_0^\infty e^{i\omega t} \langle [S_{\mathbf{q}}^z(t), S_{-\mathbf{q}}^z] \rangle dt. \quad (25)$$

Such an approximation for  $\Sigma$  has been introduced within the  $t$ - $J$  model in Ref. [22]. However, quite analogous treatment has been employed previously in the Hubbard model [15] and more recently within the spin-fermion model [19,20].

Several comments are in order to define quantities entering Eq. (25):

a) EQM (11) induce an effective spin-fermion coupling, which would emerge also from a phenomenological spin-fermion Hamiltonian with the coupling parameter  $m_{\mathbf{k}\mathbf{q}}$ , Eq. (12). In order that such a Hamiltonian is hermitian, the coupling should satisfy

$$\tilde{m}_{\mathbf{k},\mathbf{q}} = \tilde{m}_{\mathbf{k}-\mathbf{q},-\mathbf{q}}, \quad (26)$$

which is in general not the case with the form Eq. (12), therefore we use furtheron instead the symmetrized coupling

$$\tilde{m}_{\mathbf{k}\mathbf{q}} = 2J\gamma_{\mathbf{q}} + \frac{1}{2}(\epsilon_{\mathbf{k}-\mathbf{q}}^0 + \epsilon_{\mathbf{k}}^0). \quad (27)$$

Here we should point out that in contrast to previous related studies of phenomenological spin-fermion coupling [15,19,20], our  $\tilde{m}_{\mathbf{k}\mathbf{q}}$  (as well as  $m_{\mathbf{k}\mathbf{q}}$ ) is strongly dependent on both  $\mathbf{q}$  and  $\mathbf{k}$ . It is essential that in the most sensitive parts of the FS, i.e., along the AFM zone boundary ('hot' spots) where  $k = |\mathbf{Q} - \mathbf{k}|$ , the coupling is in fact quite modest determined solely by  $J$  and  $t'$ .

b) Since we are dealing with the paramagnetic state, all quantities should be spin invariant, i.e., the  $\chi^{\alpha\beta}(\mathbf{q}, \omega) =$

$\delta_{\alpha\beta} \chi(\mathbf{q}, \omega)$ . Since EQM (11) are invariant under spin rotations we have besides the  $S^z$  term analogous terms with  $S^-, S^+$ . Still we expect  $r_s = 1$  instead of  $r_s = 3$  since only the coupling to longitudinal (to local Néel spin order) spin fluctuations is considered here, while the coupling to transverse fluctuations has been already taken into account by  $\Sigma_{\text{pm}}$ .

c) In  $\Sigma_{\text{lf}}$  only the part corresponding to irreducible diagrams should enter, so there are restrictions on the proper decoupling. We will be interested mostly in the situation with a pronounced AFM short-range order where longitudinal fluctuations are slow, i.e., with the characteristic frequencies  $\omega_\kappa \lesssim 2J\kappa \ll J$ . The regime is close to that of quasistatic  $\chi(\mathbf{q}, \omega)$  where the simplest and also quite satisfactory approximation is to insert for  $\tilde{A}$  the unrenormalized  $A^0$ , the latter corresponding in our case to the spectral function without  $\Sigma_{\text{lf}}$  but with  $\Sigma = \Sigma_{\text{pm}}$ . Such an approximation has been introduced in the theory of a pseudogap in CDW systems [29], used also in related works analyzing the role spin fluctuations [15], [19], and recently more extensively examined in Ref. [30]. In the opposite case of full self-consistent treatment with  $\tilde{A} = A$  we would overcount the influence of fluctuations, although the results would probably appear not so much different as shown on simpler systems [30].

For  $\chi(\mathbf{q}, \omega)$ , Eq. (25), at  $c_h > 0$  and possibly  $T > 0$  we do not have a corresponding theory, so we treat it as an input. On one hand,  $\chi(\mathbf{q}, \omega)$  is restricted by the sum rule,

$$\frac{1}{N} \sum_{\mathbf{q}} \int_0^\infty \text{cth} \left( \frac{\beta\omega}{2} \right) \chi''(\mathbf{q}, \omega) d\omega = \frac{\pi}{4} (1 - c_h). \quad (28)$$

At the same time, the system is close to the AFM instability, so we assume spin fluctuations of the overdamped form [18]

$$\chi''(\mathbf{q}, \omega) \propto \frac{\omega}{(\tilde{q}^2 + \kappa^2)(\omega^2 + \omega_\kappa^2)}. \quad (29)$$

The appearance of the pseudogap and the form of the FS are not strongly sensitive to the particular form of  $\chi''(\mathbf{q}, \omega)$  (at given characteristic  $\kappa$  and  $\omega_\kappa$ ) provided that  $\chi(\mathbf{q}, \omega)$  is not singular as, e.g., is the case of marginal Fermi liquid scenario [13]. It has been shown [22] that the latter form is needed to get generally overdamped QP with vanishing QP weight (at  $T = 0$ ) in spectral functions at intermediate doping.

#### IV. PSEUDOGAP ANALYSIS

Full calculation of the spectral functions  $A(\mathbf{k}, \omega)$  within the presented theory requires a selfconsistent solution for  $\Sigma = \Sigma_{\text{pm}} + \Sigma_{\text{lf}}$ , where besides the model parameters  $t, t', J$  and the doping  $c_h$ , an input are also  $\mu, \kappa, \eta_1, \eta_2$ .

$\kappa, \eta_1, \eta_2$  are given by short-range spin correlations dependent mostly on  $c_h$  and can be taken from various analytical [31] and numerical [32,8] calculations within the  $t$ - $J$  model. At the same time in a selfconsistent theory  $\mu$  should be fixed via the DOS

$$\mathcal{N}(\omega) = \frac{2}{N} \sum_{\mathbf{k}} A(\mathbf{k}, \omega). \quad (30)$$

as

$$c_h = 1 - \int_{-\infty}^{\infty} f(\omega) \mathcal{N}(\omega) d\omega. \quad (31)$$

Results of such selfconsistent calculation are presented in Sec. V.

On the other hand, to establish characteristic features of the pseudogap and the development of the FS we follow first a simplified analysis. We namely notice that the effect of  $\Sigma_{\text{pm}}$  are threefold:

- a) to induce a large incoherent component in the spectral functions at  $\omega \ll 0$  in particular at low and intermediate doping,
- b) to renormalize the effective QP band relevant to the behavior at  $\omega \sim 0$  and at the FS, and
- c) to cause a transition of a large FS into a small hole-pocket-like FS at  $c_h < c_h^* \ll 1$ ,

Result b) can serve as a starting point for the discussion of the pseudogap and FS features at finite doping. If we define the effective band as

$$\begin{aligned} \epsilon_{\mathbf{k}}^{\text{ef}} &= Z_{\mathbf{k}}^{\text{ef}} [\zeta_{\mathbf{k}} + \Sigma_{\text{pm}}(\mathbf{k}, 0) - \mu], \\ Z_{\mathbf{k}}^{\text{ef}} &= \left[ 1 - \frac{\partial \Sigma_{\text{pm}}(\mathbf{k}, \omega)}{\partial \omega} \Big|_{\omega=0} \right]^{-1}, \end{aligned} \quad (32)$$

we get for the effective spectral function

$$A_{\text{ef}}^0(\mathbf{k}, \omega) = \alpha Z_{\mathbf{k}}^{\text{ef}} \delta(\omega + \mu - \epsilon_{\mathbf{k}}^{\text{ef}}), \quad (33)$$

which can be used to evaluate  $\Sigma_{\text{lf}}$ . We restrict ourselves here to the regime of intermediate (not too small) doping, where  $\epsilon_{\mathbf{k}}^{\text{ef}}$  defines the large FS.

Let us concentrate on results for  $T = 0$ . The simplest situation where  $\Sigma_{\text{lf}}$  can be evaluated analytically is the quasi-static and single-mode approximation (QSA) which is meaningful if  $\omega_{\kappa} \ll t, \kappa \ll 1$ . In this case we insert into Eq. (25)

$$\frac{1}{\pi} \chi''(\mathbf{q}, \omega) \sim \frac{1}{4} \delta(\mathbf{q} - \mathbf{Q}) [\delta(\omega - \nu) - \delta(\omega + \nu)], \quad (34)$$

with  $\nu \rightarrow 0$ . We get

$$\Sigma_{\text{lf}}^{\text{QSA}}(\mathbf{k}, \omega) = \frac{r_s m_{\mathbf{k}\mathbf{Q}}^2}{4} \frac{Z_{\mathbf{k}-\mathbf{Q}}^{\text{ef}}}{\omega - \epsilon_{\mathbf{k}-\mathbf{Q}}^{\text{ef}}} \quad (35)$$

and

$$\begin{aligned} G^{\text{QSA}}(\mathbf{k}, \omega) &= \frac{\alpha Z_{\mathbf{k}}^{\text{ef}} (\omega - \epsilon_{\mathbf{k}-\mathbf{Q}}^{\text{ef}})}{(\omega - \epsilon_{\mathbf{k}-\mathbf{Q}}^{\text{ef}})(\omega - \epsilon_{\mathbf{k}}^{\text{ef}}) - \Delta_{\mathbf{k}}^2}, \quad (36) \\ \Delta_{\mathbf{k}}^2 &= \frac{r_s}{4} Z_{\mathbf{k}}^{\text{ef}} Z_{\mathbf{k}-\mathbf{Q}}^{\text{ef}} m_{\mathbf{k}\mathbf{Q}}^2, \end{aligned}$$

The spectral functions show in this approximation two branches of  $E^{\pm}$ , separated by the gap which opens along the AFM zone boundary  $\mathbf{k} = \mathbf{k}_{\text{AFM}}$  where  $\epsilon_{\mathbf{k}-\mathbf{Q}}^{\text{ef}} = \epsilon_{\mathbf{k}}^{\text{ef}}$ . Since  $\gamma_{\mathbf{k}_{\text{AFM}}} = 0$  the relevant (pseudo)gap scale is

$$\Delta_{\mathbf{k}}^{\text{PG}} = |\Delta_{\mathbf{k}_{\text{AFM}}}| = \frac{Z_{\mathbf{k}}^{\text{ef}}}{2} \sqrt{r_s} |2J - 4t' \cos^2 k_x|. \quad (37)$$

It is instructive to realize that  $\Delta_{\mathbf{k}}^{\text{PG}}$  does not depend on  $t$ , but rather on smaller  $J$  and in particular  $t'$ . For  $t' < 0$  the gap is largest at  $(\pi, 0)$ , consistent with experiments. Whether the (pseudo)gap appears at the Fermi energy  $\omega = 0$  depends, however, on properties of  $\epsilon_{\mathbf{k}_{\text{AFM}}}^{\text{ef}}$ . We do not expect that the gap opens along the whole AFM zone boundary, since in most cases  $\epsilon_{\mathbf{k}_{\text{AFM}}}^{\text{ef}}$  crosses zero along  $(\pi/2, \pi/2)$ - $(\pi, 0)$  so that within the QSA  $E_{\mathbf{k}}^-$  forms a hole-pocket-like FS. In fact, the results of the QSA are equivalent to the system with long range spin-density-wave order (AFM), where the doubling of the unit cell appears.

Within the simplified effective band approach, Eq. (31), it is not difficult to evaluate numerically  $\Sigma_{\text{lf}}$  beyond the QSA, by taking explicitly  $\chi(\mathbf{q}, \omega)$ , Eq. (29), for  $\kappa > 0$  and  $\omega_{\kappa} = 2J\kappa$ . Integrals in Eq. (25) can be performed mostly analytically if we linearize the dependence of  $\epsilon_{\mathbf{k}}^{\text{ef}}$  within the relevant interval  $\delta k \lesssim \kappa$ .

Let us for illustration present in this Section results characteristic for the development of spectral functions with most sensitive parameters  $\kappa$  and  $\mu$ , which both simulate the variation with doping. We fix further on the model parameter  $J/t = 0.3$  as relevant for cuprates. We take here  $t'/t = -0.3$  close to values quoted for BSCCO. For simplicity we assume first that the effective band  $\epsilon_{\mathbf{k}}^{\text{ef}}$  is just renormalized  $\epsilon_{\mathbf{k}}$  (justified for an intermediate doping, see Sec. V) with fixed values  $t_{\text{ef}}/t = 0.3$ ,  $t'_{\text{ef}}/t = -0.1$  and  $Z^{\text{ef}} = 0.4$ . More realistic treatment would require the variation of latter parameters with  $c_h$  but results remain qualitatively similar. For  $\kappa$  we take in accord with experiments [1] and numerical results on the  $t$ - $J$  model [32,8,31]  $\kappa \sim \sqrt{c_h}$ .

The choice of  $\mu$  is somewhat more arbitrary since within an effective band approach the sum rule, Eq. (30), cannot be used as a criterion. Nevertheless it is evident that  $\mu$  determines the shape and the volume of the FS. In the following examples we choose  $\mu$  such that at given  $\kappa$  the DOS at the Fermi energy,  $\mathcal{N}(0)$ , reaches a local minimum. This means that effectively the states near  $(\pi, 0)$  are in the pseudogap and that the truncation of the FS is most pronounced (at given  $\kappa$ ). Such a choice of  $\mu$  in fact also yields the volume of the FS (except at extreme  $\kappa \ll 1$ ) quite close to the one consistent with the Luttinger theorem [33].

In Fig. 1 we first present results for  $A(\mathbf{k}, \omega = 0)$  at  $T = 0$  for a broad range of  $\kappa = 0.01 - 0.6$ . Curves (evaluated at small additional smearing  $\epsilon = 0.02t$ ) in fact display the effective FS determined by the condition  $G^{-1}(\mathbf{k}_F, 0) = 0$ . At the same time, intensities  $A(\mathbf{k}, \omega = 0)$  correspond to the renormalization factor  $Z_F$ . We can comment the development as follows. At extremely small  $\kappa = 0.01$  we see the hole-pocket FS which follows from the QSA in Eq. (36). In spite of small  $\kappa$  the 'shadow' side of the hole pocket has smaller  $Z_F$ . Already small  $\kappa \sim 0.05$  destroys the 'shadow' side of the pocket, i.e., the solution  $G^{-1} = 0$  on the latter side disappears since the singularity in  $\Sigma_{lf}$ , Eq. (35), is smeared out by finite  $\kappa$ . On the other hand, in the gap emerge now QP solutions with very weak  $Z_F \ll 1$  which reconnect the FS into a large one. We are dealing nevertheless with effectively truncated FS with well developed arcs. The effect of larger  $\kappa$  is essentially to increase  $Z_F$  in the gaped region, in particular near  $(\pi, 0)$ . Finally, for large  $\kappa = 0.6$  which corresponds to the regime consistent with optimal doping or overdoping in cuprates,  $Z_F$  is essentially only weakly decreasing towards  $(\pi, 0)$  and the FS is well pronounced and concave as naturally expected for  $t' < 0$ .

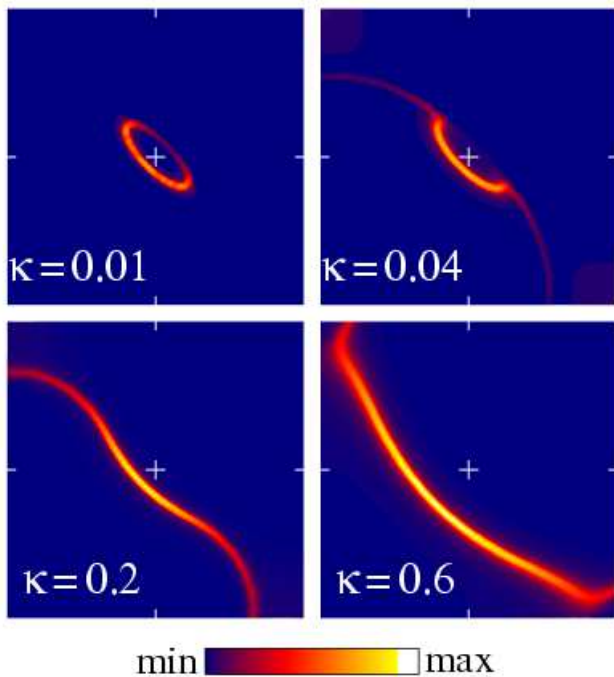


FIG. 1. (color) Contour plot of spectral functions  $A(\mathbf{k}, \omega = 0)$  at  $T = 0$  for various  $\kappa$  in one quarter of the Brillouin zone.

In order to understand the pseudogap features at low but finite  $\kappa$  we present in Figs. 2,3  $A(\mathbf{k}, \omega)$  for  $\kappa = 0.1$ . Spectra in Fig. 3 are presented along the lines a - d in the Brillouin zone as shown in Fig. 2. As expected from Eq. (36) the pseudogap is smallest along the zone diagonal (line a) where, moreover, the pseudogap appears at

$\omega > 0$ , so that it would not be seen in ARPES. Lines a and b are thus examples of the region where arcs of the FS are well pronounced, i.e., their QP weight is not strongly renormalized,  $Z_F \lesssim Z^{ef}$ . On the other hand, following lines c and d the chemical potential  $\omega = 0$  falls into the pseudogap. We see in Fig. 3(a),(b) that QP in fact crosses coherently the FS ( $\omega = 0$ ) although with very small  $Z_F \ll 1$ . It is evident from Fig. 1 that  $Z_F$  within the pseudogap remains small only for  $\kappa \ll 1$  while it increases and finally smears out the concept of the pseudogap for  $\kappa \gtrsim \kappa^* \sim 0.5$ .

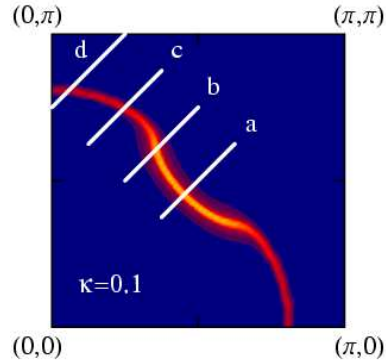


FIG. 2. (color)  $A(\mathbf{k}, \omega = 0)$  for  $\kappa = 0.1$  and lines a) - d) used in Fig. 3.

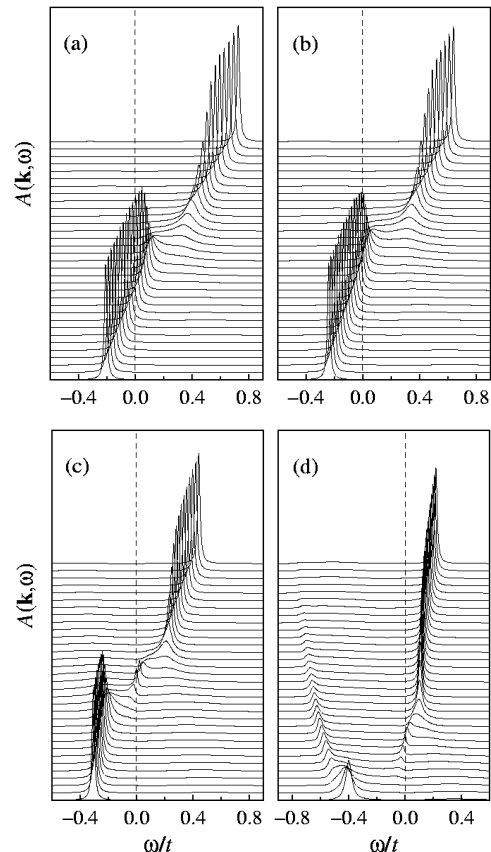


FIG. 3.  $A(\mathbf{k}, \omega)$  for  $\kappa = 0.1$  along different directions in the Brillouin zone, corresponding to Fig. 2.

It is quite remarkable to notice that in spite of  $Z_F \ll 1$  the QP velocity  $v_F$  is not diminished within the pseudogap. In fact it is even enhanced, as seen in Fig. 3(c) and even more clearly in Fig. 4 where the contour plot of  $A(\mathbf{k}, \omega)$  is shown corresponding (with restricted  $k$  span) to Fig. 3(c). Again, it is well evident in Fig. 4 that QP is well defined at the FS, while it becomes fuzzy at  $\omega \neq 0$  merging with the solutions  $E_{\mathbf{k}}^{\pm}$ , respectively, away from the FS.

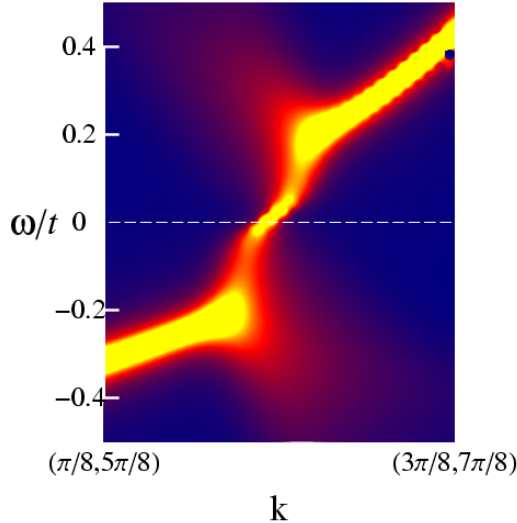


FIG. 4. (color) Contour plot of  $A(\mathbf{k}, \omega)$  for  $\kappa = 0.1$ , corresponding to Fig. 3(c). Note large quasiparticle velocity around  $\omega \sim 0$ .

Presented formalism offers a possible scenario for the evolution of the FS with doping from a pocket-like into a large one. In order to explain results in Figs. (3),(4) on the effective truncation of the FS and the character of QP within the pseudogap we note that it is essentially enough that both  $\kappa$  and  $\omega_{\kappa}$  are finite to yield well defined FS. Since gross features do not depend on the particular form Eq. (29) we present here simplified analysis using instead

$$\chi''(\mathbf{Q} + \tilde{\mathbf{q}}, \omega) = \begin{cases} C[\delta(\omega - \omega_{\kappa}) - \delta(\omega + \omega_{\kappa})], & \tilde{q}_{\perp} < \kappa, \\ 0, & \tilde{q}_{\perp} > \kappa, \end{cases} \quad (38)$$

where  $\tilde{q}_{\perp}$  denotes the component perpendicular to the AFM zone boundary. Let us assume that  $\epsilon_{\mathbf{k}}^{\text{ef}} - \mu = \epsilon \sim 0$  and  $\epsilon_{\mathbf{k}-\mathbf{Q}}^{\text{ef}} - \mu = \bar{\epsilon} \sim 0$ . We also linearize dispersion  $\epsilon_{\mathbf{k}}^{\text{ef}}$  at the FS and take that  $\mathbf{v}_{\mathbf{k}}^{\text{ef}} \parallel (1, 1)$ , so that we get from Eq. (25),

$$\Sigma(\epsilon, \omega) = -\frac{\Delta^2}{2w} \log \frac{(w + \omega_{\kappa} + \bar{\epsilon} - \omega)(\omega_{\kappa} + \omega)}{(w + \omega_{\kappa} - \bar{\epsilon} + \omega)(\omega_{\kappa} - \omega)} \quad (39)$$

where  $w = v_{\mathbf{k}}^{\text{ef}} \kappa$  and  $\Delta = \Delta_{\mathbf{k}}$ . Let us evaluate QP properties on the FS assuming that it is located at  $\bar{\epsilon} = 0$ , i.e., on the AFM zone boundary. We obtain from Eq. (39) the QP weight  $Z_F$

$$\frac{Z_F}{Z^{\text{ef}}} = \left[ 1 - \frac{\partial \Sigma'}{\partial \omega} \Big|_{\omega=0, \bar{\epsilon}=0} \right]^{-1} = \left[ 1 + \frac{\Delta^2}{\omega_{\kappa}(\omega_{\kappa} + w)} \right]^{-1}. \quad (40)$$

This clearly leads to and explains  $Z_F \ll 1$  for  $\omega_{\kappa} w \sim 2v_{\mathbf{k}}^{\text{ef}} J \kappa^2 \ll \Delta^2$ . This is generally the case within the gaped part of the FS for small  $\kappa < \kappa^*$ , as shown in Fig. 1. It should be also noted that the latter condition is essentially always satisfied near  $(\pi, 0)$  where  $v_{\mathbf{k}}^{\text{ef}} \sim 0$  and consequently also  $w \sim 0$ .

Let us evaluate in the same way the QP renormalized velocity  $v_F$  at the FS. Here we realize that the  $\mathbf{k}$  dependence of  $\Sigma'$  is essential. The latter is in Eq. (40) given by the  $\epsilon$  dependence,

$$\frac{v_F}{v_{\mathbf{k}}^{\text{ef}}} = \left( 1 + \frac{\partial \Sigma'}{\partial \epsilon} \right) \frac{Z_F}{Z^{\text{ef}}},$$

$$\frac{\partial \Sigma'}{\partial \epsilon} \Big|_{\omega=0, \bar{\epsilon}=0} = \frac{\Delta^2}{\omega_{\kappa}(\omega_{\kappa} + w)}, \quad (41)$$

which in contrast to  $Z_F$  leads to an enhancement of  $v_F$ . In the case  $\omega_{\kappa} w \ll \Delta^2$  we thus get

$$\frac{v_F}{v_{\mathbf{k}}^{\text{ef}}} \sim \frac{\omega_{\kappa}}{w} \sim \frac{2J}{v_{\mathbf{k}}}. \quad (42)$$

Final  $v_F$  is therefore not strongly renormalized, since  $2J$  and  $v_{\mathbf{k}}^{\text{ef}}$  are of similar order. Furthermore,  $\tilde{v}_F$  is enhanced in the parts of FS where  $v_{\mathbf{k}}^{\text{ef}}$  is small, in particular near  $(\pi, 0)$  point. The situation is thus very different from 'local' theories where  $\Sigma(\mathbf{k}, \omega) \sim \Sigma(\omega)$  and the QP renormalization is governed only by  $Z_F$ . In our case the 'non-local' character of  $\Sigma(\mathbf{k}, \omega)$  is essential in order to properly describe QP within the pseudogap region.

Let us discuss further the behavior of the DOS  $\mathcal{N}(\omega)$ , Eq. (30). It is evident from Fig. 1 that the contribution to  $\mathcal{N}(\omega \sim 0)$  will come mostly from FS arcs near the zone diagonal while the gaped regions near  $(\pi, 0)$  will contribute less. Results in Fig. 5 (full lines) the development of  $\mathcal{N}(\omega)$  with  $\kappa$ , as corresponding to FS in Fig. 1. We see that the DOS indeed reveal a pseudogap at  $\omega < \Delta$  however the pseudogap is visible only for  $\kappa < 0.5$  and deepens for  $\kappa \rightarrow 0$ .

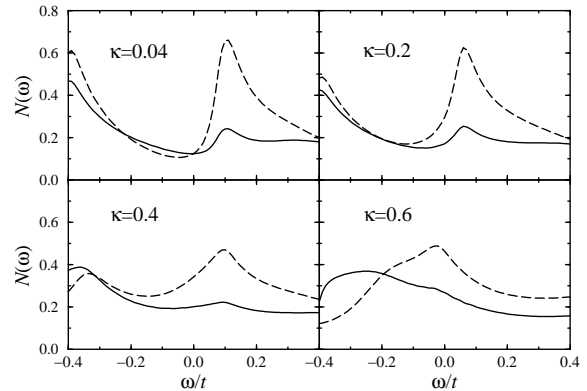


FIG. 5. Density of states  $\mathcal{N}(\omega)$  (full lines) and weighted DOS  $\mathcal{N}_w(\omega)$  (dashed lines) for different  $\kappa$ .

The DOS is measured in cuprates via angle integrated PES, e.g. for LSCO in [34], as well as via the scanning tunneling microscopy (STM) [35]. It is well possible that within both experiments the matrix elements are essential leading to enhanced contribution near the x points in the Brillouin zone. It has been proposed that for the  $c$ -axis conductivity [36] the interplanar hopping should be weighted by the matrix element

$$w(\mathbf{k}) = (\cos k_x - \cos k_y)^2. \quad (43)$$

The same arguments as for the  $c$ -axis conductivity might apply also for the STM effective DOS as well as for integrated PES, therefore we present also the weighted DOS  $\mathcal{N}_w$  where  $w(\mathbf{k})$  is introduced additionally into Eq. (30). Results also presented in Fig. 5 (dashed line) show much stronger pronounced pseudogap, in particular at low  $\kappa$ . This is quite evident since  $w(\mathbf{k})$  essentially destroys the effect of FS arcs near  $(\pi/2, \pi/2)$  which present the main contribution (due to small velocity in hole-pocket FS) to the usual  $\mathcal{N}(\omega)$ .

In Fig. 6(a) we show the average  $Z_{\text{av}}$  along the FS, as well as the QP DOS, defined as

$$\mathcal{N}_{QP} = \frac{\alpha Z^{\text{ef}}}{2\pi^2} \oint \frac{dS_F}{v(\mathbf{k})}. \quad (44)$$

in Fig. 6(b) we present as well as the dependence of DOS at the FS, both  $\mathcal{N}(0)$  and  $\mathcal{N}_w(0)$ , as a function of  $\kappa$ . Note that  $\mathcal{N}_{QP}$  should be relevant for the specific heat, i.e.,  $\mathcal{N}_{QP} \propto \gamma = C_V/T$  at low  $T$  (provided that we are dealing with a normal Fermi liquid). It is quite important to understand that decreasing  $\kappa$  (smaller doping) also means the decrease of  $\mathcal{N}_{QP}$ , which is consistent with the observation of the pseudogap also in the specific heat in cuprates [37]. We note here that such a behavior is not evident when one discusses the metal-insulator transition. Namely, in a Fermi liquid with (nearly) constant Fermi surface one can drive the metal-insulator transition by  $Z_{\text{av}} \rightarrow 0$  and within an assumption of a local character  $\Sigma(\omega)$  this would lead to  $v_F \rightarrow 0$  and consequently to  $\mathcal{N}_{QP} \rightarrow \infty$ . Clearly, the essential difference in our case is that within the pseudogap regime  $\Sigma(\mathbf{k}, \omega)$  is nonlocal, allowing for the simultaneous decrease of  $\mathcal{N}(0)$  and  $\mathcal{N}_{QP}$ .

Finally, let us comment on the influence of finite  $T$ . While  $T$  enters within this approach also via effective parameters as  $v_{\mathbf{k}}^{\text{ef}}$  and predominantly  $\kappa(T)$ , here we consider only the direct effect via the thermodynamic factor in Eq. (25). It is evident that  $T > 0$  smears out  $\Sigma_{\text{lf}}$ . This becomes important at small  $\kappa$  in particular for QP in the pseudogap regime. In Fig. 7 we present  $A(\mathbf{k}, \omega)$ , corresponding to Fig. 3(c), for several values of low  $T$ . The main conclusion is, that weak (but sharp) QP peak with  $Z_F \ll 1$  at  $T = 0$  is smeared out already by very small  $T > T^s \sim 0.02t$  and is not at all visible (there is no overdamped peak) at higher  $T$ , the remainder being an incoherent background at  $\omega \sim 0$  for  $T > T^s$ . This is

important to realize that ARPES experiments in fact do not observe no well defined QP peak near  $(\pi, 0)$  in the underdoped regime at  $T > T_c$ .

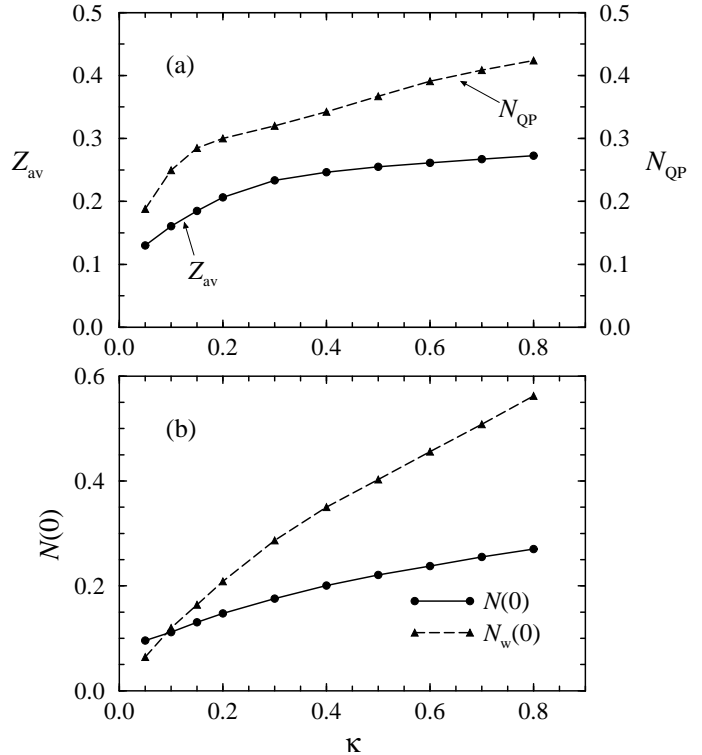


FIG. 6. (a) Average QP weight  $Z_{\text{av}}$  and QP DOS  $\mathcal{N}_{QP}$  vs.  $\kappa$ . (b) DOS  $\mathcal{N}(0)$  and weighted DOS  $\mathcal{N}_w(0)$  vs.  $\kappa$ .

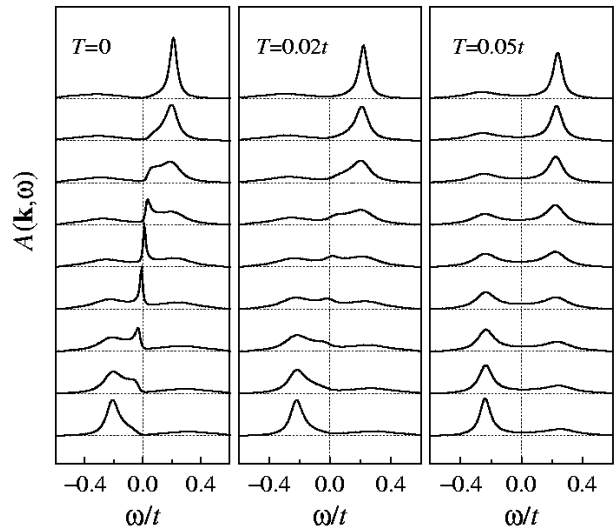


FIG. 7.  $A(\mathbf{k}, \omega)$  for  $\kappa = 0.1$  and  $\mathbf{k}$  along the central part of the line  $c$  in Fig. 2 for various  $T$ :  $T = 0$ ,  $T = 0.02t$ , and  $T = 0.05t$ . Momentum  $\mathbf{k}$  ranges from  $(\pi/4, 3\pi/4) \mp (\pi/32, \pi/32)$ .

## V. SELF CONSISTENT CALCULATION

The full selfconsistent set of equations for  $\Sigma = \Sigma_{\text{pm}} + \Sigma_{\text{lf}}$ , Eqs.(22),(25), and for  $G$ , Eq.(15), is solved numerically. For given  $\mu$  the FS emerges as a solution determined by the relation  $\zeta_{\mathbf{k}_F} + \Sigma'(\mathbf{k}_F, 0) = \mu$ . We should note that at given  $\mu$ , electron concentration  $c_e$  as calculated from the DOS  $\mathcal{N}(\omega)$ , Eq.(31), does not in general coincide with the one evaluated from the FS volume,  $\tilde{c}_e = V_{\text{FS}}/V_0$ . Nevertheless, apart from the fact that within the  $t$ - $J$  model validity of the Luttinger theorem is anyhow under question [38], in the regimes of large FS both quantities appear to be quite close. The position of the FS is mainly determined by  $\zeta_{\mathbf{k}}$  and  $\Sigma_{\text{pm}}$ , while in this respect  $\Sigma_{\text{lf}}$  is less crucial.

As discussed in Sec. III we use in Eq. (7) the most appropriate and simplest approximation to insert the unrenormalized  $A^0(\mathbf{k}, \omega)$ , i.e., the spectral function without a self-consistent consideration of  $\Sigma_{\text{lf}}$  but with  $\Sigma_{\text{pm}}$  fully taken into account. We choose here  $t' = -0.2t$  and again  $\kappa = \sqrt{c_h}$  while  $\eta_1$  and  $\eta_2$  are determined as a function of  $c_h$  from model calculations [32]. We use  $N = 40 \times 40$  points in the Brillouin zone and broadening  $\epsilon/t = 0.05$ .

In Fig. 8 we present hole concentration  $c_h$  vs.  $\mu$  as obtained from  $\mathcal{N}(\omega)$  at  $T = 0$ . We solve selfconsistent equations by iteration, whereby for  $0.06 < c_h < 0.11$  we find in the equations an instability signaled by oscillatory behavior instead of the convergence and an unique solution can not be obtained in the region indicated by the dashed line. However, at lower (and higher) doping the solution is converged. It seems that the region of instability coincides with the transition from the large to a small FS.

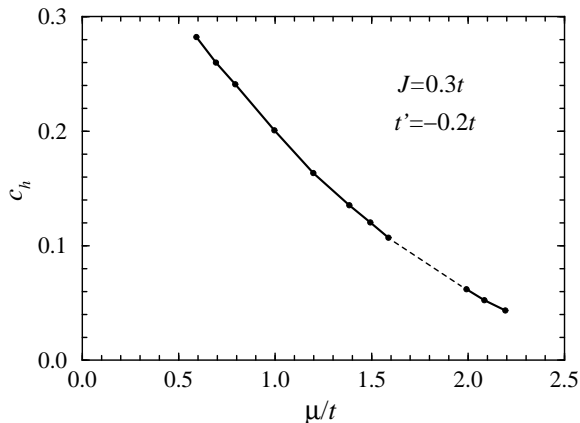


FIG. 8. Hole doping  $c_h$  as a function of the chemical potential  $\mu/t$ , following from the selfconsistent calculation.

The shape of the FS is most clearly presented with contour plot of the electron momentum distribution function defined as

$$\tilde{n}(\mathbf{k}) = \alpha^{-1} \int_{-\infty}^0 A(\mathbf{k}, \omega) d\omega. \quad (45)$$

Results for a characteristic development of the FS with  $c_h$  are shown in Fig. 9. At higher doping,  $c_h = 0.26$  and also  $c_h = 0.20$ , we get a common large FS topology. In the intermediate doping regime,  $c_h = 0.14$ , the pseudogap is pronounced at momenta around  $(\pi, 0)$  and the FS shows a tendency of forming a small FS. The gap is more pronounced because of longer AFM correlation length  $\xi$  (smaller  $\kappa$ ). At  $c_h < c_h^0 \sim 0.06$  solutions are consistent with a small pocket-like FS whereby this behavior is enhanced by  $t' < 0$  as realized in other model studies [9]. On increasing doping the FS rather abruptly changes from a small into a large one as suggested from the results of the SCBA [39]. The smallness of  $c_h^0$  has the origin in quite weak dispersion dominated by  $J$  and  $t'$  at  $c_h \rightarrow 0$  which is overshadowed by much larger  $\zeta_{\mathbf{k}}$  at moderate doping, where the FS is large and its shape is controlled by  $t'/t$ .

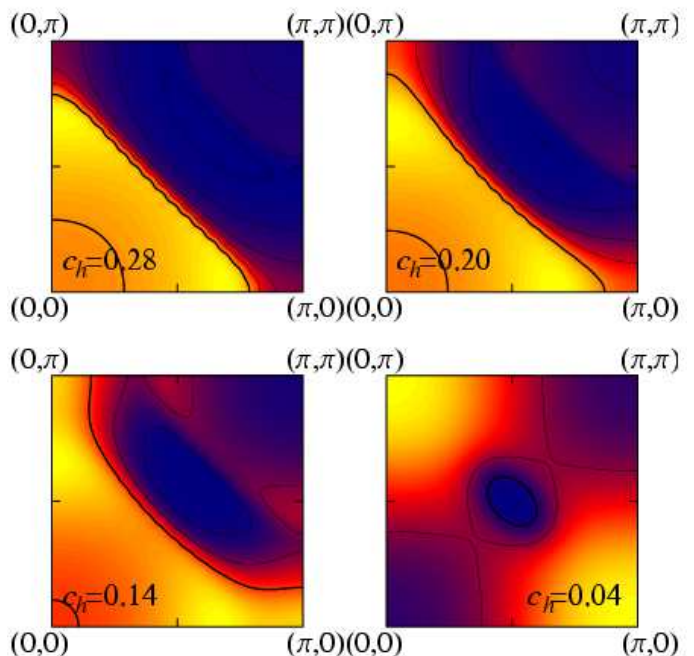


FIG. 9. (color) Electron momentum distribution  $\tilde{n}(\mathbf{k})$  for various  $c_h$ . Thin contour lines represent  $\tilde{n}(\mathbf{k})$  in increments 0.1 while heavy line is corresponding to  $\tilde{n}(\mathbf{k}) = 0.8$  for  $c_h = 0.26, 0.20, 0.14$  and  $\tilde{n}(\mathbf{k}) = 0.85$  for  $c_h = 0.04$ .

In Fig. 10(a) and Fig. 10(b) we present calculated  $A(\mathbf{k}, \omega)$  along the principal directions in the Brillouin zone, i.e.,  $(\pi/2, \pi/2) \rightarrow (0, 0) \rightarrow (\pi, 0)$ . It is evident that  $\Sigma_{\text{pm}}$  leads to a strong damping of hole QP and quite incoherent momentum-independent spectrum  $A(\mathbf{k}, \omega)$  for  $\omega \ll -J$  which qualitatively reproduces ARPES and numerical results [12]. Electron QP (at  $\omega > 0$ ) are in general very different, i.e., with much weaker damping aris-

ing only from  $\Sigma_{\text{pm}}$ . Note a relatively high QP velocity in the higher doping regime  $c_h = 0.26$ , Fig. 10(a), as compared to a more narrow dispersion on the scale  $2J$  at low doping  $c_h = 0.04$ , Fig. 10(b), where we find the regime of small pocket-like FS.

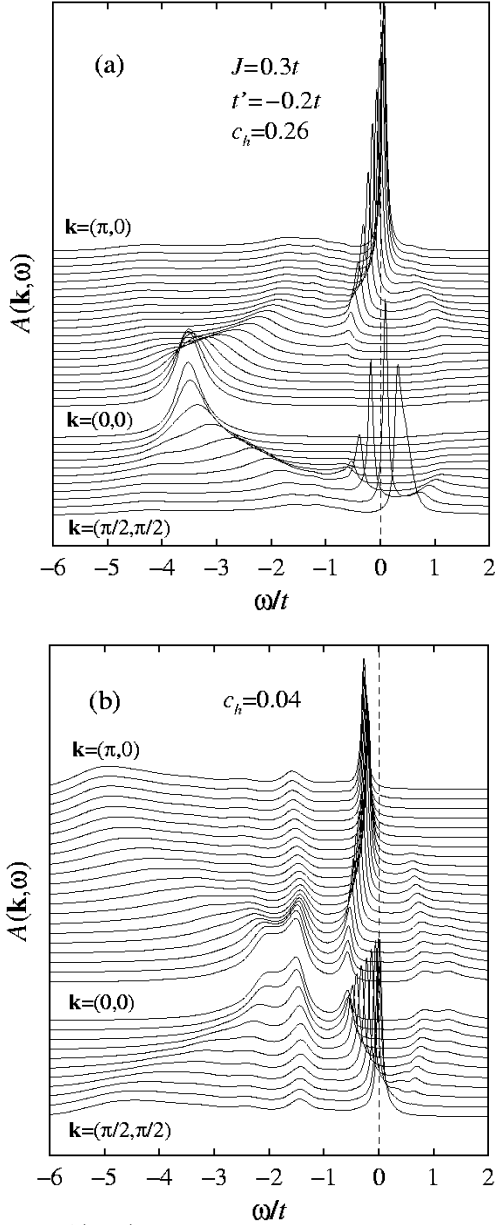


FIG. 10.  $A(\mathbf{k}, \omega)$  along main directions in the Brillouin zone.

In Fig. 11 we present the development of spectral functions at fixed  $c_h = 0.2$ , but now varying  $\kappa$  as an independent parameter. Let us concentrate on the emergence of the pseudogap near  $(\pi, 0)$ . At  $\kappa = 0.4 \sim \sqrt{c_h}$  the pseudogap is essentially not yet developed. Nevertheless, the gap opens with decreasing  $\kappa$ , in particular for (at this doping unrealistic value)  $\kappa = 0.05$ .

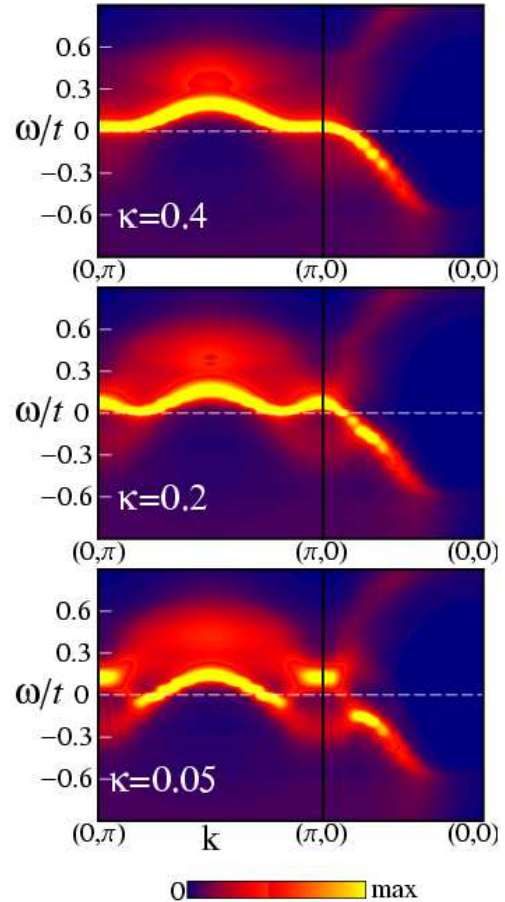


FIG. 11. (color) Contour plot of  $A(\mathbf{k}, \omega)$  for fixed doping  $c_h = 0.2$  and various  $\kappa$ .

## VI. CONCLUSIONS

We have presented the theory of spectral functions within the  $t$ - $J$  model whereby our method is based on the EQM for projected fermionic operators and on the decoupling approximation for the self energy assuming the fermions and spin fluctuations as essential coupled degrees of freedom. We first make some comments on the method:

- The EQM approach for spectral functions (as well as for other dynamical quantities) seem to be promising since it can treat exactly the constraint which is essential for the physics of strongly correlated electrons.
- In finding the proper approximation for the self energy within the EQM approach it is plausible that the main coupling is of fermions with spin fluctuations, where close to the AFM ordered state both transverse and longitudinal spin fluctuations are important. It is well possible, however, that other contributions could be important, e.g., the coupling to pairing fluctuations.
- In an ordered AFM our method reproduces naturally the results for the spectral function (of a hole) within SCBA, which is highly nontrivial, since both approaches

are quite different.

d) The coupling to longitudinal spin fluctuations appear to be most important for QP near the AFM zone boundary and is responsible for the opening of the pseudogap. Here the coupling is only moderately strong and can be treated in the lowest-order decoupling scheme.

e) The present theory uses the spin response as an input.  $\chi''(\mathbf{q}, \omega)$ , Eq.(29), corresponds in general to a Fermi liquid or to a short-range AFM liquid. Results remain in fact qualitatively similar as far as  $\chi''(\mathbf{q}, \omega)$  is nonsingular. In the opposite case, e.g., if we would use the MFL form as an input, the Fermi surface would still be defined, but QP would have vanishing weight  $Z \rightarrow 0$  [22].

Let us further discuss some main results of the presented theory:

a) The fermion-paramagnon coupling as manifested in  $\Sigma_{\text{pm}}$  remains effective and strong even at moderate doping. The full calculation shows that the coupling leads to a large incoherent part in the hole part ( $\omega < 0$ ) of the spectral function, as well as to the renormalized band  $\epsilon_{\mathbf{k}}^{\text{ef}}$ .

b) The main consequence of  $\Sigma_{\text{lf}}$  due to the coupling to longitudinal spin fluctuations is the appearance of the pseudogap at  $\kappa < \kappa^*$ . The pseudogap opens predominantly along the AFM zone boundary and its extent is qualitatively given by Eq.(37), dependent on  $J$  and  $t'$  but not directly on  $t$ . Evidently the pseudogap has similarity to d-wave-like dependence along the FS, for  $t' < 0$  being largest near the  $(\pi, 0)$  point.

c) How strong is the pseudogap effect depends mainly on  $\kappa$ . At small  $\kappa \ll \kappa^*$  parts of the Fermi surface near  $(\pi/2, \pi/2)$  remain well pronounced (for  $t' < 0$ ) while the Fermi surface within the pseudogap is suppressed, i.e., QP have a small weight  $Z_F \ll 1$ , in particular near zone corners  $(\pi, 0)$ .

d) The simplified analysis yields large Fermi surface, although a truncated one, except at very small  $\kappa \ll \kappa^*$  where  $\Sigma_{\text{lf}}$  by itself induces a small hole-pocket-like Fermi surface. On the other hand,  $\Sigma_{\text{pm}}$  generates hole pockets already for  $c_h < c_h^0 \sim 0.06$ . In fact, an instability of the self consistent calculation indicates the emergence of hole-pocket Fermi surface even at  $c_h \lesssim 0.1$ . However, it is well possible that within the present approximation scheme  $\Sigma_{\text{pm}}$  is overestimated at intermediate  $c_h$ , an indication for that being quite a weak dispersion  $\epsilon_{\mathbf{k}}^{\text{ef}}$ .

e) Our method is approximative in the evaluation of  $\Sigma$ , hence it is not surprising that the volume of the Fermi surface does in general not coincide with the one following the Luttinger theorem. It is anyhow questionable if such a relation should be valid within the  $t$ - $J$  model [38] due to the projected basis and strong correlations. Nevertheless, in the regime of a large Fermi surface the full calculation yields the Fermi surface volume quite close to the Luttinger one.

f) For  $\kappa < \kappa^*$  the QP within the pseudogap have small weight  $Z_F \ll 1$  but not diminished  $v_F$ , which is the effect of the nonlocal character of  $\Sigma(\mathbf{k}, \omega)$ . A consequence is

that QP within the pseudogap contribute much less to QP DOS  $\mathcal{N}_{QP}$ . This can explain the reduction of the latter with doping and the appearance of the pseudogap in the specific heat being essential for the understanding of the specific heat in underdoped cuprates.

g) Although most results are presented for  $T = 0$ , we can discuss some effects of  $T > 0$ . First effect is that within the pseudogap the QP with  $Z_F \ll 1$  are washed out (not just overdamped) already for very small  $T < T^s \ll \Delta^{PG}$ . On the other hand, the pseudogap is mainly affected by  $\kappa$ . So we can argue that the pseudogap would be observable for  $\kappa(c_h, T) < \kappa^* \sim 0.5$ . This effectively determines the pseudogap crossover temperature  $T^*(c_h)$ . From the quantitative studies of the  $t$ - $J$  model [40,31] it appears that in the region of interest  $\kappa$  is nearly linear in both  $T$  and  $c_h$  so we would get approximately

$$T^* \sim T_0^*(1 - c_h/c_h^*), \quad (46)$$

where  $T_0^* \sim 0.6J$  and  $c_h^* \sim 0.15$ .

Finally we make some comments on the relevance of our results to experiments on cuprates, in particular with respect to observed pseudogap and Fermi surface features:

a) The (large) pseudogap scale shows in ARPES on BSCCO as a hump at  $\sim 100\text{eV}$  [2]. Our results indicate quite a similar pseudogap scale, e.g. in Fig. 5 the  $\omega < 0$  pseudogap  $\sim 0.3 t$  (note that  $t \sim 0.4\text{eV}$ ), since  $\Delta^{PG}$  is determined mainly by  $J$  and  $t'$ .

b) The truncated Fermi surface in underdoped BSCCO appears as an arc (part of the large Fermi surface corresponding to  $t' < 0$ ) in the Brillouin zone [3], effectively not crossing the AFM zone boundary, which is also characteristic of our results for  $\kappa < \kappa^*$ , originating from the strong coupling to spin fluctuations with commensurate  $(\pi, \pi)$ . The same is the origin of shadow features in spectral functions pronounced at intermediate doping and in particular at weak doping.

c) Our results for the depletion of the DOS  $\mathcal{N}(0)$  ( $\mathcal{N}_w(0)$ ) with decreasing doping are qualitatively consistent with the integrated PES (so far known for LSCO [34]) and STM [35], although in this relation the importance of matrix element corrections is not yet clarified. The same holds for the calculated decrease of QP DOS  $\mathcal{N}_{QP}$  with doping essential in connection with the specific-heat pseudogap in underdoped cuprates [37]. It should be however mentioned that our results for both  $\mathcal{N}(0)$  as well as of  $\mathcal{N}_{QP} \propto \gamma$  indicate on weaker suppression with decreasing doping than observed in experiments. This is due to remaining contribution of Fermi surface arcs, which could be overestimated in our approach for  $\kappa \ll \kappa^*$ .

d) Both the value and the dependence of the pseudogap temperature  $T^*(c_h)$ , as estimated in Eq.(46), seem to be very reasonable in connection with experimental evidence, arising from various transport and magnetic properties in cuprates [1].

- 
- [1] for a review see, e.g., M. Imada, A. Fujimori, and Y. Tokura, *Rev. Mod. Phys.* **70**, 1039 (1998).
- [2] D.S. Marshall *et al.*, *Phys. Rev. Lett.* **76**, 4841 (1996); H. Ding *et al.*, *Nature* **382**, 51 (1996).
- [3] M.R. Norman *et al.*, *Nature* **392**, 157 (1998).
- [4] A. Fujimori *et al.*, in *Proc. of the NATO ARW on Open Problems in Strongly Correlated Electron Systems*, Eds. J. Bonča, P. Prelovšek, A. Ramšak, and S. Sarkar (Kluwer, Dordrecht, 2001), p. 119.
- [5] C.L. Kane, P. A. Lee, and N. Read, *Phys. Rev. B* **39**, 6880 (1989); G. Martínez and P. Horsch, *Phys. Rev. B* **44**, 317 (1991); A. Ramšak and P. Prelovšek, *Phys. Rev. B* **42**, 10415 (1990).
- [6] B. O. Wells *et al.*, *Phys. Rev. Lett.* **74**, 964 (1995).
- [7] F. Ronning *et al.*, *Science* **282**, 2067 (1998).
- [8] For a review, see E. Dagotto, *Rev. Mod. Phys.* **66**, 763 (1994).
- [9] T. Tohyama and S. Maekawa, *J. Phys. Soc. Jpn.* **59**, 1760 (1990); *Supercond. Sci. Technol.* **13** R17 (2000).
- [10] W. Stephan and P. Horsch, *Phys. Rev. Lett.* **66**, 2258 (1991).
- [11] J. Jaklič and P. Prelovšek, *Phys. Rev. B* **55**, R7307 (1997); P. Prelovšek, J. Jaklič, and K. Bedell, *Phys. Rev. B* **60**, 40 (1999).
- [12] for a review see J. Jaklič and P. Prelovšek, *Adv. Phys.* **49**, 1 (2000).
- [13] C.M. Varma, P.B. Littlewood, S. Schmitt-Rink, E. Abrahams, and A.E. Ruckenstein, *Phys. Rev. Lett.* **63**, 1996 (1989).
- [14] R. Preuss, W. Hanke, C. Gröber, and H.G. Evertz, *Phys. Rev. Lett.* **79**, 1122 (1997).
- [15] A. Kampf and J.R. Schrieffer, *Phys. Rev. B* **41**, 6399 (1990).
- [16] N. E. Bickers, D. J. Scalapino, and S. R. White, *Phys. Rev. Lett.* **62**, 961 (1989); M. Langer, J. Schmalian, S. Grabowski, and K. H. Bennemann, *Phys. Rev. Lett.* **75**, 4508 (1995).
- [17] Z. Wang, Y. Bang, and G. Kotliar, *Phys. Rev. Lett.* **67**, 2733 (1991).
- [18] P. Monthoux, A.V. Balatsky, and D. Pines, *Phys. Rev. Lett.* **67**, 3448 (1991); *Phys. Rev. B* **46**, 14803 (1992); P. Monthoux and D. Pines, *Phys. Rev. B* **47**, 6069 (1993).
- [19] A.V. Chubukov and D.K. Morr, *Phys. Rep.* **288**, 355 (1997).
- [20] J. Schmalian, D. Pines, and B. Stojković, *Phys. Rev. Lett.* **80**, 3839 (1998); *Phys. Rev. B* **60**, 667 (1999).
- [21] D. Zanchi and H.J. Schulz, *Europhys. Lett.* **44**, 235 (1997); N. Furukawa, T.M. Rice, and M. Salmhofer, *Phys. Rev. Lett.* **81**, 3195 (1998).
- [22] P. Prelovšek, *Z. Phys. B* **103**, 363 (1997).
- [23] N.M. Plakida and V.S. Oudovenko, *Phys. Rev. B* **59**, 11949 (1999).
- [24] S. Onoda and M. Imada, *J. Phys. Soc. Jpn.* **70**, 632 (2001).
- [25] P. Prelovšek and A. Ramšak, *Phys. Rev. B* **63**, 180506 (2001).
- [26] D. N. Zubarev, *Sov. Phys. Usp.* **3**, 320 (1960).
- [27] H. Mori, *Prog. Theor. Phys.* **33**, 423 (1965).
- [28] W. Götze and P. Wölfle, *Phys. Rev. B* **6**, 1226 (1972).
- [29] P.A. Lee, T.M. Rice, and P.W. Anderson, *Phys. Rev. Lett.* **31**, 462 (1973).
- [30] A.J. Millis and H. Monien, *Phys. Rev. B* **61**, 12496 (2000).
- [31] R.R.P. Singh and R.L. Glenister, *Phys. Rev. B* **46**, 11871 (1992).
- [32] J. Bonča, P. Prelovšek, and I. Sega, *Europhys. Lett.* **10**, 87 (1989).
- [33] J. M. Luttinger, *Phys. Rev.* **119**, 1153 (1960).
- [34] A. Ino *et al.*, *Phys. Rev. Lett.*, **81**, 2124 (1998).
- [35] Ch. Renner, B. Revaz, K. Kadowaki, I. Maggio-Aprile, and O. Fischer, *Phys. Rev. Lett.* **80**, 3606 (1998).
- [36] L.B. Ioffe and A.J. Millis, *Phys. Rev. B* **58**, 11631 (1998).
- [37] J.W. Loram, K.A. Mirza, J.R. Cooper, and W.Y. Liang, *Phys. Rev. Lett.* **71**, 1740 (1993); J.W. Loram, J.L. Luo, J.R. Cooper, W.Y. Liang, and J.L. Tallon, *Physica C* **341 - 8**, 831 (2000).
- [38] W.O. Putikka, M.U. Luchini, and R.R.P. Singh, *Phys. Rev. Lett.* **81**, 2966 (1998).
- [39] A. Ramšak, I. Sega, and P. Prelovšek, *Phys. Rev. B* **61**, 4389 (2000).
- [40] A. Sokol, R.L. Glenister, and R.R.P. Singh, *Phys. Rev. Lett.* **72**, 1549 (1994).